Mechanism for a Pairing State with Time-Reversal Symmetry Breaking in Iron-Based Superconductors

Christian Platt[1], Ronny Thomale[1,2,3], Carsten Honerkamp[4], Shou-Cheng Zhang[3], and Werner Hanke[1]
[1] *Theoretical Physics, University of Würzburg, D-97074 Würzburg*
[2] *Department of Physics, Princeton University, Princeton, NJ 08544*
[3] *Department of Physics, McCullough Building, Stanford University, Stanford, California 94305-4045 and*
[4] *Institute for Theoretical Solid State Physics, RWTH Aachen University and*
JARA - FIT Fundamentals of Future Information Technology, D-52056 Aachen
(Dated: June 30, 2011)

The multipocket Fermi surfaces of iron-based superconductors promote pairing states with both $s_{\pm}$-wave and $d_{x^2-y^2}$-wave symmetry. We argue that the competition between these two order parameters could lead to a time-reversal-symmetry breaking state with $s+id$-pairing symmetry in the iron-based superconductors, and propose serveral scenarios in which this phase may be found. To understand the emergence of such a pairing state on a more rigorous footing, we start from a microscopic 5-orbital description representative for the pnictides. Using a combined approach of functional renormalization group and mean-field analysis, we identify the microscopic parameters of the $s+id$-pairing state. There, we find the most promising region for $s+id$-pairing in the electron doped regime with an enhanced pnictogen height.

PACS numbers: 74.20.Mn, 74.20.Rp, 74.25.Jb, 74.72.Jb

Iron based superconductors (SC) offer an appealing platform to investigate the interplay among pairing interactions, pairing symmetries and Fermi surface topologies [1]. Generally, repulsive interactions in momentum space can lead to a change of sign in the pairing amplitude. A large class of iron based SC have disconnected Fermi surface pockets, consisting of hole pockets at the $\Gamma=(0,0)$ and possibly $M=(\pi,\pi)$ points, and two electron pockets at the $X=(\pi,0)/(0,\pi)$ points in the unfolded Brillouin zone (BZ) with one iron atom per unit cell. When the repulsive interactions between the hole and the electron pockets dominate, an $s_{\pm}$ pairing symmetry can be obtained [2–4]. On the other hand, when the repulsive interactions between the two electron pockets dominate, a propensity toward d-wave pairing symmetry can be expected. When both types of interactions are comparable, there is hence a frustration between the two pairing symmetry types. A recent theoretical proposal suggests that the system can resolve the frustration by a pairing state with the $s+id$ pairing symmetry which spontaneously breaks time-reversal (TR) symmetry [5]. The possibility of a TR-symmetry breaking pairing state due to frustrating pairing interactions among three or more Fermi pockets has also been investigated in several other contexts [6–10]. In general, time reversal breaking pairing states have rather accessible experimental signatures, and several proposals have been suggested in the context of iron based SC [5].

In principle there are various experimentally tunable parameters to drive the competition between s-wave and d-wave in the pnictides, giving the opportunity to start from both limits. In $K_xBa_{1-x}Fe_2As_2$, the Fermi surface topology can be chosen as a paradigmatic setup for $s_{\pm}$, consisting of hole pockets at Γ and the electron pockets at X for optimal doping $x\simeq 0.4$. For increasing x, however, the electron pockets decrease, and have nearly disappeared for $x=1$ [Fig. 1], which has been recently suggested to host a d-wave pairing symmetry [11]. In this system, it is hence plausible that a $s+id$ pairing state can be realized for intermediate values of x. In the chalcogenide $K_xFe_{2-y}Se_2$, the electron pockets at the X points dominate, and, for a situation seemingly inverse to KFe_2As_2, a d-wave pairing symmetry may likewise be expected [12, 13]. (It should be noted that the actual pairing symmetry in the chalcogenides is far from settled, as a strong coupling perspective may likewise suggest $s_{\pm}$ pairing [14].) By tuning doping or other possible parameters affecting the band structure such as pressure, one possibly induces a pocket at Γ, increasing the tendency towards $s_{\pm}$ pairing symmetry [Fig. 1]. In this case,

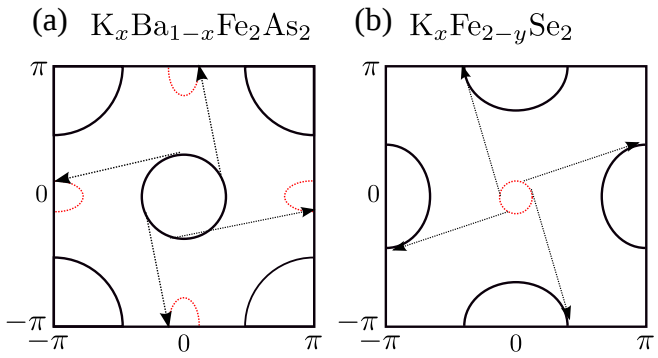

FIG. 1. (Color online). Frustrating the d-wave limits of KFe_2As_2 (a) and $K_xFe_{2-y}Se_2$ (b). Upon doping or differently induced band structure effects, electron pockets appear (dashed red) in (a) and a hole pocket appears (dashed red) in (b) which populate the $q\sim(\pi,0)/(0,\pi)$ scattering channels enhancing the $s_{\pm}$ symmetry. This leads to frustration providing the background for $s+id$ pairing.

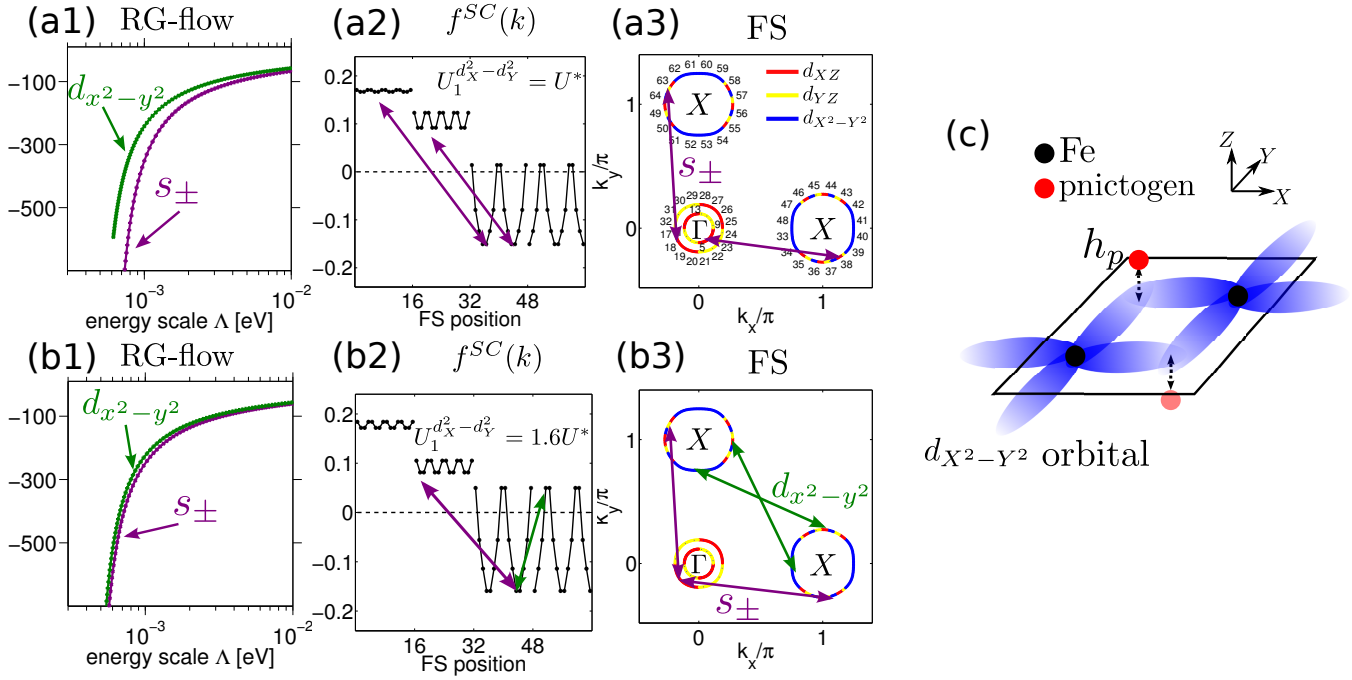

FIG. 2. (Color online). Competing pairing orders and SC form factors for $U_1(d_{X^2-Y^2}) = U_1^* = 2.5eV$ (a) and $U_1(d_{X^2-Y^2}) = 1.6U^*$ (b) at electron doped filling $n = 6.13$. RG channel flow (a1,b1) and $s_\pm$-gap form factor (a2,b2). $s_\pm/d_{x^2-y^2}$ transition from (a) to (b): increasing $U_1(d_{X^2-Y^2})$ enhances the gap anisotropy of the $s_\pm$-form factor on the electron pockets [$\boldsymbol{k}$-patching: points 33-64 see (a3)] shown in (a2,b2) until its symmetry switches to $d_{x^2-y^2}$. (a3,b3) Interactions mediated by U_1, setting up the $s_\pm$-pairing tendency between hole pockets and electron pockets ($\Gamma \leftrightarrow X$) and the competing $d_{x^2-y^2}$-pairing symmetry due to electron-electron ($X \leftrightarrow X$) interaction. (c) The variation of the pnictogen height h_p particularly affects the spread of the $d_{X^2-Y^2}$-orbital and therefore $U_1(d_{X^2-Y^2})$, as it is oriented to the planar projection of the pnictogen.

one could also expect an $s + id$ pairing state. By systematically tuning the Fermi pocket topologies, one can compare the predicted pairing symmetries with experiments, and determine the nature of the pairing interaction by these investigations, starting from compound settings with a suspected d-wave symmetry [Fig. 1].

In the following, we rather intend to start from an $s_\pm$ pairing state to begin with, and address how we can enhance the competitiveness of the d-wave symmetry to drive the system into the $s + id$ regime. The reason for this is two-fold. First, the $s_\pm$ symmetry is much more generic for the different classes of pnictides. Second, as we will see below, we find the most promising setup to be located on the electron doped side of pnictides, where high-quality samples have already been grown for different families. We hence believe that this regime may be the experimentally most accessible scenario at the present stage, which is why we explicate it in detail. In this paper, we investigate the microscopic mechanism of the $s+id$ pairing state by the functional renormalization group (fRG) method of a five band model. We systematically vary the doping level and the strength of intra-orbital interaction, which determine the ratio between the electron-hole pocket and the electron-electron pocket mediated pairing interactions. In this microscopic investigation, we find that the $s + id$ pairing state can be realized in the intermediate electron-doped regime, given that we also adjust the pnictogen height parameter of the system appropriately.

We start from a representative 5-band model for the pnictides which is obtained from LDA-type calculations [3]. It has been considered by us before as a starting point for explaining the difference between the isovalent P-based and As-based pnictides [15]. The LDA "non-interacting" part is given by

$$H_0 = \sum_{\boldsymbol{k},s} \sum_{a,b=1}^{5} c^\dagger_{\boldsymbol{k}as} K_{ab}(\boldsymbol{k}) c_{\boldsymbol{k}bs}. \qquad (1)$$

Here c's stand for electron annihilation operators, a, b for the d-orbitals, s denotes the spin indices and $K_{ab}(\boldsymbol{k})$ the orbital (i.e. maximally-localized Wannier function) ma-

trix elements of the Kohn-Sham Hamiltonian. The band structure features electron pockets at X and hole pockets at Γ, which is the typical situation in the pnictides [Fig. 2] for sufficient electron doping. The many-body interaction part is given by the intra- and inter-orbital interactions U_1 and U_2, as well as the Hund's coupling $J_{\rm H}$ and the pair hopping $J_{\rm pair}$:

$$H_{\rm int} = \sum_i \Bigg[U_1 \sum_a n_{i,a\uparrow} n_{i,a\downarrow} + U_2 \sum_{a<b,s,s'} n_{i,as} n_{i,bs'} + \sum_{a<b} (J_{\rm H} \sum_{s,s'} c^\dagger_{ias} c^\dagger_{ibs'} c_{ias'} c_{ibs} + J_{\rm pair} c^\dagger_{ia\uparrow} c^\dagger_{ia\downarrow} c_{ib\downarrow} c_{ib\uparrow}) \Bigg], \quad (2)$$

where $n_{i,as}$ denote density operators at site i of spin s in orbital a. Typical interaction settings are dominated by intra-orbital coupling, $U_1 > U_2 > J_{\rm H} \sim J_{\rm pair}$. In the fRG [15–20], one starts from the bare many-body interaction (2) in the Hamiltonian. The pairing is dynamically generated by systematically integrating out the high-energy degrees of freedom including important fluctuations (magnetic, SC, screening, vertex corrections) on equal footing. This differs from the RPA which takes right from the outset a magnetically driven SF-type of pairing interaction. For a given instability characterized by some order parameter $\hat{O}_{\mathbf{k}}$, the effective interaction vertex $V_\Lambda(\mathbf{k}_1, \mathbf{k}_2, \mathbf{k}_3, \mathbf{k}_4)$ in the particular ordering channel can be written in shorthand notation as $\sum_{\mathbf{k},\mathbf{p}} V_\Lambda(\mathbf{k}, \mathbf{p}) [\hat{O}^\dagger_{\mathbf{k}} \hat{O}_{\mathbf{p}}]$. Accordingly, the effective interaction vertex $V_\Lambda(\mathbf{k}, -\mathbf{k}, \mathbf{p}, -\mathbf{p}))$ in the Cooper channel can be decomposed into different eigenmode contributions [15, 16]

$$V^{\rm SC}_\Lambda(\mathbf{k}, \mathbf{p}) = \sum_i c^{\rm SC}_i(\Lambda) f^{{\rm SC},i}(\mathbf{k})^* f^{{\rm SC},i}(\mathbf{p}), \quad (3)$$

where i is a symmetry decomposition index, and the leading instability of that channel corresponds to an eigenvalue $c^{\rm SC}_1(\Lambda)$ first diverging under the flow of Λ. $f^{{\rm SC},i}(\mathbf{k})$ is the SC form factor of pairing mode i which tells us about the SC pairing symmetry and hence gap structure associated with it. In the fRG, from the final Cooper channel in the effective interaction vertex, this quantity is computed along the discretized Fermi surfaces [Fig. 2(a3)], and the leading SC instabilities are plotted in Figs. 2(a1) and (b1). The interaction parameters are kept fixed at the representative setup $U_1 = 2.5eV, U_2 = 2.2eV, J_{\rm H} = 1.2eV, J_{\rm pair} = 0.2eV$ (U_1 for the $d_{X^2-Y^2}$-orbital is varied as explicitly stated in Figs. 2 and 3). The relatively large bare value of J_H is motivated partly by recent findings, in particular, for a sizable Hund's rule coupling [21, 22]. Furthermore, as a parameter trend, larger J_H and smaller $J_{\rm pair}$ tends to prefer the $s + id$-phase in the electron-doped regime for rather moderate values of intra-orbital coupling U_1 [Fig. 3].

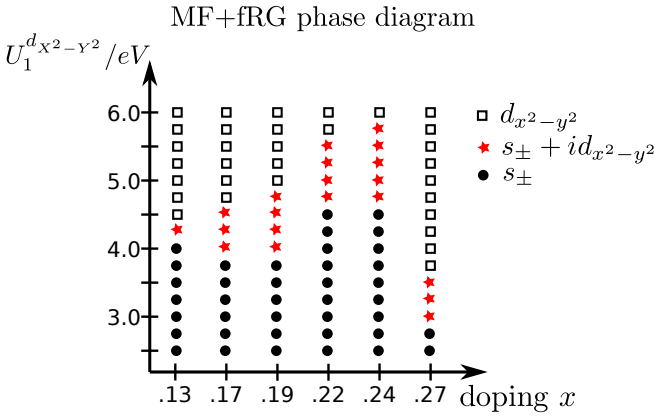

FIG. 3. (Color online). Preferred pairing as a function of electron doping and intra-orbital Coulomb interaction $U_1(d_{X^2-Y^2})$. The results are obtained by minimizing the mean-field free energy of the effective theory taken from fRG at $\Lambda \approx .001eV$. At 27% electron doping, the $s + id$-pairing state occurs at $U_1(d_{X^2-Y^2}) = 3eV$ which is comparable to the intra-orbital repulsion in the remaining orbitals $U_1 = 2.5eV$.

The situation in Fig. 2 is representative for moderate electron doping and interaction scales of the pnictides, where the $\Gamma \leftrightarrow X$ pair scattering between the hole pockets at Γ and the electron pockets at X dominates. Already from the BCS gap equation, a finite momentum transfer can induce pairing only when the wave vector of such an interaction connects regions on one FS (such as in the cuprate case), or regions on different FSs (such as in the pnictide case), which have opposite signs of the SC order parameter. This corresponds to putting the electron pairs in an anisotropic wave function such as sign-reversing s-wave ($s_\pm$) in Fig. 2a, where the wave vector $(\pi, 0)$ in the unfolded BZ connects hole and electron pockets with a sign-changing $s_\pm$ gap [2, 4]. However, in the fRG calculation of Fig. 2b with increased U_1 interaction on the $d_{X^2-Y^2}$ orbital, a green arrow for $X \leftrightarrow X$ scattering indicates additional interactions that become similarly important as the $(\pi, 0)$ channel. This increased U_1 can be tuned by the pnictogen height as explained below and frustrates the previous "pure" $s_\pm$ limit ($\Gamma \to X$). The system then strikes a compromise [15, 23] by enhancing the anisotropy of the formfactor (denoted by $f^{\rm SC}(\mathbf{k})$ in Fig. 2) on the electron pockets at X. The multi-band SC hence adjusts the momentum dependence of the gap, i.e. its anisotropy, so as to minimize the effect of the Coulomb repulsion which is set up by the competition between $s_\pm$ and $d_{x^2-y^2}$-wave channels.

We now have all ingredients to tune the pairing symmetry from $s_\pm$-wave to $d_{x^2-y^2}$-wave and, eventually, into the TR-symmetry broken $s + id$ phase. In most of the iron-based SC, the tendency towards $s_\pm$-pairing occurs slightly more pronounced than the competing $d_{x^2-y^2}$-pairing and, at first glance, the resulting frustration appears to be too small for causing $s + id$-pairing. There-

fore, in order to increase frustration, we somehow have to enhance the pair-scattering between the electron pockets at X which then promotes the sub-leading $d_{x^2-y^2}$-channel. As shown in a-priori determinations of the interaction in Eq. (2), expressed in terms of orbital matrix elements, the pnictogen height h_p (measured from the Fe-plane [Fig. 2c]) has a substantial influence on the intra-orbital interaction U_1 between $d_{X^2-Y^2}$-Wannier orbitals [24], which can be either modified by isovalent doping or pressure. By increasing h_p, the Wannier functions in this orbital are further localized, causing an increase of $U_1(d_{X^2-Y^2})$. In Fig. 2b, we have already used this fact to demonstrate that, for moderate e-doping (13%), large values of this matrix element drive the SC instability from $s_{\pm}-$ to $d_{x^2-y^2}$-wave symmetry.

For this setup, we present our predictions for TR-symmetry breaking in a schematic phase diagram in Fig. 3, where we plot the leading $s_{\pm}$, $d_{x^2-y^2}$ and finally $s+id$ SC solutions as a function of $U_1(d_{X^2-Y^2})$, and electron doping. There, we have used our fRG result as a starting point for a renormalized mean field analysis [25]. In this MF+fRG approach, the one-loop flow is stopped at a scale Λ which is small compared to the bandwidth, but still safely above the scale Λ_c, where the 2-particle vertex diverges. In this range, the particular choice of the cutoff Λ does not significantly influence the results in Fig. 3. The renormalized coupling function $V^{\Lambda}(\boldsymbol{k}_1,\boldsymbol{k}_2,\boldsymbol{k}_3,\boldsymbol{k}_4)$ is taken as an input for the mean field treatment of the remaining modes. As shown in Fig. 2, the regime of $s_{\pm}/d$-wave pairing competition features a single channel SC instability without other competing (e.g. magnetic) instabilities and, therefore, justifies

$$V^{\Lambda}(\boldsymbol{k}_1,\boldsymbol{k}_2,\boldsymbol{k}_3,\boldsymbol{k}_4) \approx V^{pair}(\boldsymbol{k}_1,\boldsymbol{k}_3)\delta_{\boldsymbol{k}_2,-\boldsymbol{k}_1}\delta_{\boldsymbol{k}_4,-\boldsymbol{k}_3}, \quad (4)$$

with $V^{pair}(\boldsymbol{k}_1,\boldsymbol{k}_3) = V^{\Lambda}(\boldsymbol{k}_1,-\boldsymbol{k}_1,\boldsymbol{k}_3,-\boldsymbol{k}_3)$. The effective theory for quasiparticles near the Fermi surface ($|\xi(\boldsymbol{k})|<\Lambda$) is modeled by the reduced Hamiltonian

$$H^{\Lambda} = \sum_{\boldsymbol{k}s}\xi(\boldsymbol{k})c^{\dagger}_{\boldsymbol{k}s}c_{\boldsymbol{k}s} + \frac{1}{N}\sum_{\boldsymbol{k},\boldsymbol{q}}V^{pair}(\boldsymbol{k},\boldsymbol{q})c^{\dagger}_{\boldsymbol{k}\uparrow}c^{\dagger}_{-\boldsymbol{k}\downarrow}c_{-\boldsymbol{q}\downarrow}c_{\boldsymbol{q}\uparrow}, \quad (5)$$

where $\xi(\boldsymbol{k})$ is taken as the bare dispersion due to only weak band-renormalization effects. The MF solution of this reduced Hamiltonian is obtained as in BCS theory, by solving the self-consistent gap-equation and calculating the corresponding grand potential which is

$$\Omega^{stat} = -\sum_{\boldsymbol{k}}\frac{|\Delta_{\boldsymbol{k}}|^2+2\xi(\boldsymbol{k})^2}{2\sqrt{\xi(\boldsymbol{k})^2+|\Delta_{\boldsymbol{k}}|^2}} + \sum_{\boldsymbol{k}}\xi(\boldsymbol{k}). \quad (6)$$

Within a reasonable range of parameters for the electron-doped pnictides, we then find a regime favoring $s+id$-pairing due to

$$\Omega^{stat}_{s+id} < \Omega^{stat}_{s_{\pm}}, \Omega^{stat}_{d}. \quad (7)$$

Note, that this phase regime is only a lower bound for the existence of $s+id$ which probably is much larger. This is because the fRG setup at present only allows us to obtain the leading SC instability at some finite Λ_c, while the $s+id$ phase may well set in below Λ_c. This would manifest itself as a change of the SC phase as a function of temperature.

In summary, we have presented a microscopic analysis, based on a-priori electronic structure determinations and a combination of the fRG with an MF treatment of the remaining low-energy states, to derive a kind of "guiding principle" for a possible $s+id$ pairing state in the pnictides. For the case of increased electron doping and pnictogen height, we have illustrated how this drives the system into an $s+id$ SC state. Aside from this example, other regimes in the pnictides likewise promise the possible realization of an $s+id$ state, such as hole-doped (K,Ba)-122 interpolating between the s-wave limit ($x\sim 0.4$) and d-wave limit ($x\sim 1$) as well as possibly the chalcogenides $K_xFe_{2-y}Se_2$.

We thank A. V. Chubukov, D. Scalapino, and P. Hirschfeld for discussions. CP, RT, CH and WH are supported by DFG-SPP 1458/1, CP, CH and WH by DFG-FOR 538. RT is supported by the Humboldt Foundation.

[1] Y. Kamihara *et al.*, J. Am. Chem. Soc. **130**, 3296 (2008).
[2] I. I. Mazin, D. J. Singh, M. D. Johannes, and M. H. Du, Phys. Rev. Lett. **101**, 057003 (2008).
[3] K. Kuroki, S. Onari, R. Arita, H. Usui, Y. Tanaka, H. Kontani, and H. Aoki, Phys. Rev. Lett. **101**, 087004 (2008).
[4] A. V. Chubukov, D. V. Efremov, and I. Eremin, Phys. Rev. B **78**, 134512 (2008).
[5] W. C. Lee, S. C. Zhang and C. Wu, Phys. Rev. Lett. **102**, 217002 (2009).
[6] D. F. Agterberg, V. Barzykin and L. P. Gorkov, Phys. Rev. B **60**, 14868 (1999), and refs. therein.
[7] T. K. Ng and N. Nagaosa, Europhys. Lett. **87**, 17003 (2009).
[8] V. Stanev and Z. Tesanovic, Phys. Rev. B **81**, 134522 (2010).
[9] Y. Tanaka and T. Yanagisawa,, J. Phys. Soc. Jpn. **79**, 1147061 (2010).
[10] X. Hu and Z. Whang, arXiv:1103.0123v2.
[11] R. Thomale, C. Platt, J. Hu, W. Hanke, and B. A. Bernevig, arXiv:1101.3593.
[12] T. A. Maier, S. Graser, P. J. Hirschfeld, and D. J.Scalapino, arXiv:1101.4988.
[13] F. Wang, F. Yang, M. Gao, Z.-Y. Lu, T. Xiang, and D.-H. Lee, Europhy. Lett. **93**, 57003 (2011).
[14] C. Fang, Y.-L. Wu, R. Thomale, B. A. Bernevig, and J. Hu, arXiv:1105.1135
[15] R. Thomale, Ch. Platt, W. Hanke and A. Bernevig, Phys. Rev. Lett. **106**, 187003 (2011).
[16] F. Wang, H. Zhai, Y. Ran, A. Vishwanath, and D.-H. Lee, Phys. Rev. Lett **102**, 1047005 (2009)
[17] R. Thomale, C. Platt, J. Hu, C. Honerkamp, and B. A.

Bernevig, Phys. Rev. B **80**, 180505 (2009)
[18] C. Platt, C. Honerkamp, and W. Hanke, New J. Phys. **11**, 055058 (2009).
[19] C. Honerkamp, M. Salmhofer, N. Furukawa, and T. M. Rice, Phys. Rev. B **63**, 035109 (2001)
[20] W. Metzner, M. Salmhofer, C. Honerkamp, V. Meden and K. Schoenhammer, arXiv:1105.5289
[21] J. Zhang, R. Sknepnek, M. Fernandes and Jörg Schmalian, Phys. Rev. B **79**, 220502(R) (2009)
[22] K. Haule and G. Kotliar, New J. Phys. **11**. 02502 (2009)
[23] C. Platt, R. Thomale, and W. Hanke, arXiv:1012.1763.
[24] For a recent review see M. Imada and T. Miyake, ch.5.2.6, J. Phys. Soc. Jpn. **79**, 112001 (2010)
[25] J. Reiss, D. Rohe, W. Metzner, Phys. Rev. B **75**, 075110 (2007)